Inorganic Chemistry

Article

pubs.acs.org/IC

Effects of Doping on Transport Properties in Cu–Bi–Se-Based Thermoelectric Materials

Jae-Yeol Hwang,[†,◇] Hyeon A. Mun,[‡,◇] Sang Il Kim,[§] Ki Moon Lee,[§] Jungeun Kim,[∥,⊥] Kyu Hyoung Lee,*[,#] and Sung Wng Kim*[,†,‡]

[†]Center for Integrated Nanostructure Physics, Institute for Basic Science (IBS), Sungkyunkwan University, Suwon 440-746, Korea

[‡]Department of Energy Science, Sungkyunkwan University, Suwon 440-746, Korea

[§]Materials R&D Center, Samsung Advanced Institute of Technology, Samsung Electronics, Suwon 443-370, Korea

[∥]Japan Synchrotron Radiation Research Institute, Hyogo 679-5198, Japan

[⊥]RIKEN SPring-8 Center, Kouto, Sayo-cho, Hyogo 679-5148, Japan

[#]Department of Nano Applied Engineering, Kangwon National University, Chuncheon 200-701, Korea

Supporting Information

ABSTRACT: The thermoelectric properties of Zn-, In-, and I-doped $Cu_{1.7}Bi_{4.7}Se_8$ pavonite homologues were investigated in the temperature range from 300 to 560 K. On the basis of the comprehensive structural analysis using Rietveld refinement of synchrotron radiation diffraction for $Cu_{x+y}Bi_{5-y}Se_8$ compounds with the inherently disordered crystallographic sites, we demonstrate a doping strategy that provides a simultaneous control for enhanced electronic transport properties by the optimization of carrier concentration and exceptionally low lattice thermal conductivity by the formation of point defects. Substituted Zn or In ions on Cu site was found to be an effective phonon scattering center as well as an electron donor, while doping on Bi site showed a moderate effect for phonon scattering. In addition, we achieved largely enhanced power factor in small amount of In doping on Cu site by increased electrical conductivity and moderately decreased Seebeck coefficient. Coupled with a low lattice thermal conductivity originated from intensified point defect phonon scattering by substituted In ions with host Cu ions, a thermoelectric figure of merit ZT of 0.24 at 560 K for $Cu_{1.6915}In_{0.0085}Bi_{4.7}Se_8$ was achieved, yielding 30% enhancement compared with that of a pristine $Cu_{1.7}Bi_{4.7}Se_8$ at the same temperature.

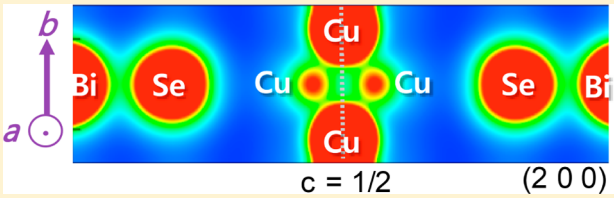

INTRODUCTION

Exploring semiconducting materials with complex structure has been widely demonstrated as a promising route to develop new materials with a high thermoelectric (TE) figure of merit, $ZT = S^2\sigma T/\kappa$ (where S, σ, κ, and T denote the Seebeck coefficient, electrical conductivity, thermal conductivity, and absolute temperature), since a low lattice thermal conductivity (κ_{lat}) originates in the structural complexity.[1,2] On the basis of this strategy, we found a new n-type pavonite homologue $Cu_{x+y}Bi_{5-y}Se_8$ ($1.2 \le x \le 1.5$, $0.1 \le y \le 0.4$) TE compound with an intrinsically low κ_{lat} (0.41–0.55 W m^{-1} K^{-1} at 300 K) derived from an inherently disordered structure, which is highlighted with the interstitial Cu and substitutional Cu on Bi sites followed by the displacement of Se sites.[3] Maximum ZT value of 0.27 at 560 K was obtained through compositional tuning for adjusting the site occupancy and carrier concentration (n_c); however, the moderate power factor (PF, $S^2\sigma$) prevents the achievement of a higher TE performance.[3] A substitutional doping approach has been the most general way to improve the PF by optimization of n_c. Because the carrier transport properties such as Hall mobility (μ_H), carrier relaxation time (τ), and effective mass (m^*) are largely affected by the change of n_c through substitutional doping associated with the change of carrier scattering mechanisms, the optimization of n_c by a precise control is the prerequisite requirement for maximizing PF. Further, the substitutional doping reduces the κ_{lat} due to the point defect phonon scattering originated from the mass difference between host atoms and dopants.[4,5]

However, the accurate prediction of the changes of electronic and thermal transport properties in complexly structured materials associated with the substitutional doping are complicated because there are difficulties in clarifying the role of structural factors (such as atomic and ionic disorders, structural distortion, and/or various crystallographic sites of constituent atoms) on the TE properties. Thus, the establishment of doping strategies is a vital issue in complexly structured TE materials for enhancing the ZT value, and the understanding of electronic structures as well as lattice dynamics based on the structural analysis is the key to conceive the strategies.

Here we report the doping effects on the electronic and thermal transport properties of pavonite homologue $Cu_{x+y}Bi_{5-y}Se_8$ compounds. A systematic doping strategy by the comprehensive structural analysis was provided to clarify the

Received: June 23, 2014
Published: November 17, 2014

   dx.doi.org/10.1021/ic5014945 | Inorg. Chem. 2014, 53, 12732–12738

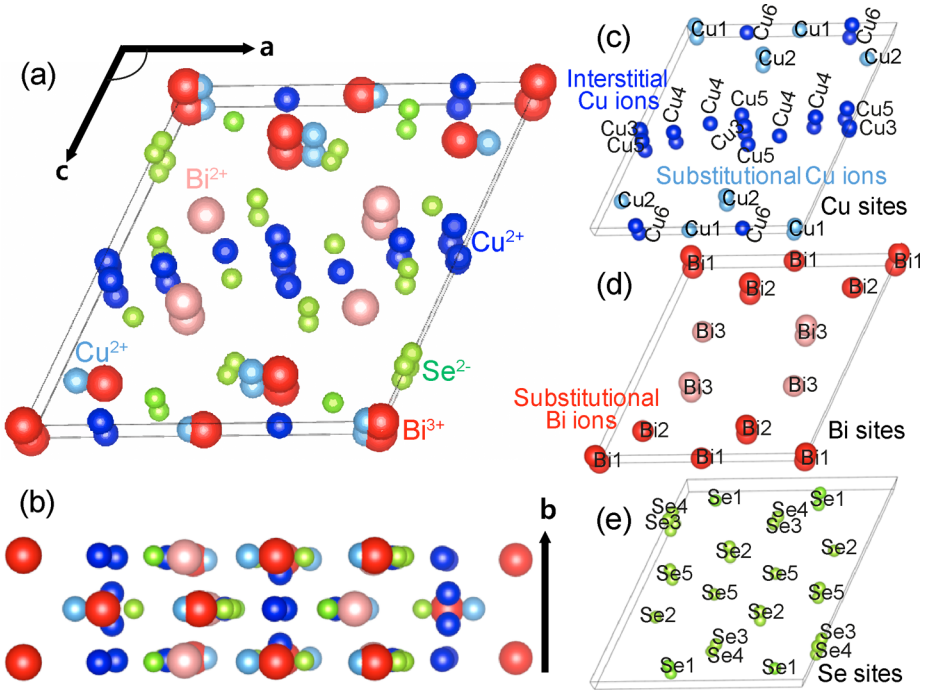

Figure 1. (a) Crystal structure and (b) the (0 0 1) view of $Cu_{x+y}Bi_{5-y}Se_8$. All distinguishable atomic sites for Cu, Bi, and Se in the unit cell were visualized in (c), (d), and (e), respectively.

uncertainties relating to their transport properties. First, the structural characteristics of each atomic site for $Cu_{1.3}Bi_{4.9}Se_8$, $Cu_{1.7}Bi_{4.7}Se_8$, and $Cu_{1.9}Bi_{4.6}Se_8$ were analyzed using Rietveld refinement of synchrotron radiation diffractions. Then, we selected $Cu_{1.7}Bi_{4.7}Se_8$ as a material for demonstration of doping effects and designed the compositions with doping elements for both substitutional and interstitial sites by considering the results of structural analysis including valence state, site occupancy, charge distribution, and bonding characteristics. It was demonstrated that an extremely low κ_{lat} value of 0.32 W m^{-1} K^{-1} was achieved by Zn doping on Cu site, and the largest ZT of 0.24 at 560 K was obtained in $Cu_{1.6915}In_{0.0085}Bi_{4.7}Se_8$ due to the synergetic effects of increase in PF by tuning n_c and decrease in κ_{lat} by intensified point defect phonon scattering on interstitial sites.

EXPERIMENTAL SECTION

Sample Preparation. Crystal ingots of $Cu_{x+y}Bi_{5-y}Se_8$ ($(x, y) = (1.2, 0.1)$, $(1.4, 0.3)$, and $(1.5, 0.4)$), Zn- and In-doped $Cu_{1.7}Bi_{4.7}Se_8$ ($Cu_{1.7-u}M_uBi_{4.7}Se_8$ and $Cu_{1.7}Bi_{4.7-v}M_vSe_8$, M = Zn and In, u and v = 0.0085 and 0.025, respectively), and I-doped $Cu_{1.7}Bi_{4.7}Se_8$ compounds ($Cu_{1.7}Bi_{4.7}Se_{8-w}I_w$, w = 0.08 and 0.16) were fabricated through the conventional melting technique by use of high-purity elemental Cu (99.999%, CERAC), Bi (99.999%, 5N Plus), Se (99.999%, 5N Plus), Zn (99.999%), In (99.999%), and I (99.999%) as starting materials. The stoichiometric mixtures of the elements were loaded into a quartz tube of 14 mm in diameter. The tube was vacuum-sealed, and the mixed contents were melted in a furnace for 10 h at 1273 K; then they were water-quenched. The ingots were ground using ball mill, and compacted bulk samples of 10 mm in diameter and 13 mm in thickness were prepared using spark plasma sintering (SPS) technique under dynamic vacuum and with the application of 50 MPa of uniaxial pressure at 663 K. The relative densities of the resulting consolidated samples were found to range from 7.22 to 7.48 g cm^{-3}, which are more than 95% of the theoretical value.

Electronic and Thermal Transport Properties. The electronic transport properties including σ and S were measured from 300 to 560 K using an ULVAC ZEM-3 system. The κ values ($\kappa = \rho_s C_p \lambda$) were calculated from measurements taken separately: sample density (ρ_s), heat capacity (C_p), and thermal diffusivity (λ) measured under vacuum by laser-flash method (TC-9000, ULVAC, Japan), in which C_p was used as the constant value of 0.225 J g^{-1} K^{-1} estimated from the Dulong–Petit fitting using low-temperature C_p data (see calculation in Supporting Information, S1). All measured data, which were acquired at the same dimension and configuration, are obtained within the experimental error of ~5%.

Synchrotron X-ray Diffractions and Rietveld Refinements. Room-temperature synchrotron powder diffraction measurements were carried out at the beamline BL02B2 at SPring-8 (Japan) using a large Debye–Sherrer camera with an image plate detector. The incident X-ray wavelength (λ = 0.354 97 Å) with horizontal polarization was determined by calibration on a standard CeO_2 sample (a = 5.411 102 Å). The data were acquired from $2\theta = 1.5°$ to $2\theta = 50°$ with a step size of 0.01°. Owing to the small diameter of the capillary (0.1 mm) and the high energy of the incoming X-rays, absorption and extinction are negligible. For the Rietveld refinement, FULLPROF suite was used, and structure factors were extracted after successive refinements with different structural models at the condition of convergence with the best pattern match.[6]

RESULTS AND DISCUSSION

The Structural Characteristics of Atomic Sites in $Cu_{x+y}Bi_{5-y}Se_8$. Figure 1a,b shows the crystal structure of monoclinic $Cu_{x+y}Bi_{5-y}Se_8$ with the space group $C2/m$, which can be described as a sandwich structure of "accreting" and "non-accreting" slabs (namely, a nonaccreting slab is sandwiched between two accreting slabs along the c-axis). One accreting slab centered at $c = 0$ has two trivalent octahedral sites of a central Bi1 and a marginal Bi2, and Bi2 is connected with the other adjacent slab. It is noteworthy that the nonstoichiometric structural formula of $Cu_{x+y}Bi_{5-y}Se_8$ compounds is caused by partial substitution of Bi sites by Cu atoms.[3] Two trivalent Bi sites are partially substituted by divalent Cu (Cu1 for Bi1 and Cu2 for Bi2 sites), and the neighboring Se atom position is split into two positions of Se3 and Se4. Minor Cu6 is also positioned in this slab. The non-accreting slab centered at $c = 1/2$ is composed of

dx.doi.org/10.1021/ic5014945 | Inorg. Chem. 2014, 53, 12732–12738

fully occupied octahedral divalent Bi3 and complex occupation by interstitial Cu atoms (Cu3, Cu4, and Cu5) surrounding the random distribution of Se5 atoms. The 14 atomic sites of Cu, Bi, and Se in a unit cell are summarized in Supporting Information (Table S1). For the engineering of electronic and thermal transport properties in this complex structure by doping approach, the fundamentals of the structural characteristics for each atomic site including atomic position, bonding, and charge valence should be clarified.

To address this issue, the Rietveld refinements of high-resolution synchrotron powder diffractions were performed for three compositions of $Cu_{1.3}Bi_{4.9}Se_8$, $Cu_{1.7}Bi_{4.7}Se_8$, and $Cu_{1.9}Bi_{4.6}Se_8$ as shown in Figure 2. For a high accuracy of

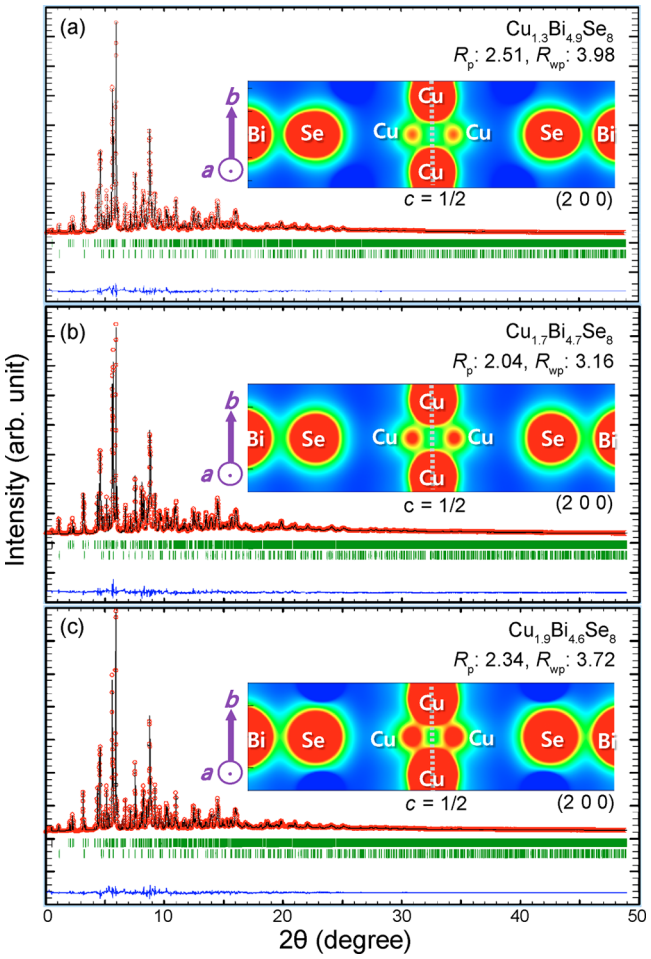

Figure 2. Refinement results of Rietveld analyses for (a) $Cu_{1.3}Bi_{4.9}Se_8$, (b) $Cu_{1.7}Bi_{4.7}Se_8$, and (c) $Cu_{1.9}Bi_{4.6}Se_8$ pavonite homologues. Synchrotron XRD patterns (black line), calculated patterns (red circle), calculated Bragg peak positions (green) for primary (up) and secondary (down: Bi_2Se_3) phases, and residual, which is the difference between measured and calculated patterns (blue). Measured range is from 1.5° to 50° in 2θ. (inset) The charge densities on the (2 0 0) planes for each compound.

refinements between experimental and calculated diffraction patterns, thermal displacement parameters were refined first under the fixed occupancies followed by the refinement of occupancy for each atom considering three structural constraints: (i) the divalent Bi site (Bi3) is fully occupied, (ii) the total occupancies of Se is 4, and (iii) the sum of occupancy for substitutional Bi (Bi1 and Bi2) and Cu (Cu1 and Cu2) sites is less than unity. Refinement results are summarized in Supporting Information (Tables S1 and S2). Note that the occupancies of the interstitial Cu sites (Cu3−Cu6) considerably increased with increasing Cu content in $Cu_{x+y}Bi_{5-y}Se_8$, whereas the occupancies of substitutional Cu sites were almost same with altering Cu/Bi ratio. This indicates that Cu ions are favorable to occupy the interstitial atomic sites rather than the substitutional ones in this structure. Total occupancy ratio (Occ_{int}/Occ_{sub}) between interstitial (Occ_{int}) and substitutional (Occ_{sub}) Cu sites were 11.26, 15.04, and 16.92 for $Cu_{1.3}Bi_{4.9}Se_8$, $Cu_{1.7}Bi_{4.7}Se_8$, and $Cu_{1.9}Bi_{4.6}Se_8$, respectively. Both lattice constants and the value of β angle were slightly changed maintaining the similar volume with varying Cu/Bi ratio. Interestingly, the lattice parameter of b decreased with increasing Cu content, while the value of β angle increased. This implies that the lattice distortion and atomic disordering are relevant to the configuration of Cu ions (that is, the occupancy of interstitial Cu sites). Thus, a large structural change can be induced by the impurity doping on the interstitial Cu sites together, leading to the expectation of a dramatic change in TE transport properties. The simulated charge density distributions of the (2 0 0) planes based on the structure refinements are represented in the insets of Figure 2. The charge densities of four interstitial Cu ions at $c = 1/2$ are overlapping each other along the b-axis, and the degree of charge density overlapping between the interstitial Cu ions depends on the occupancy of interstitial Cu, resulting in the change in the lattice parameter of b. This is correlated with the change in electronic transport properties, since the interstitial Cu sites along b-axis become a conduction path, leading to an improvement of electron transfer across the basal plane.[3] Additionally, interstitial Cu sites distributed in a zigzag pattern along b-axis can effectively scatter (or block) the heat-carrying phonon between alternating slabs. Indeed, the highest σ and the lowest κ values were observed in $Cu_{1.9}Bi_{4.6}Se_8$ with highest Cu content.[3] This strongly suggests that the interpretation of structural characteristics can predict the changes of electronic and thermal transport properties by doping at interstitial sites.

(a). Divalent Substitutional Cu (Cu1 and Cu2) and Interstitial Cu Site (Cu3, Cu4, Cu5, and Cu6). Cu sites in $Cu_{x+y}Bi_{5-y}Se_8$ can be categorized into two types in terms of coordination number and site occupancy shared with adjacent Bi sites (Figure 1c). Substitutional Cu sites (Cu1 and Cu2, azure) share the occupancy with the nearest neighbor Bi1 or Bi2 sites. Otherwise, the others are interstitial Cu sites (Cu3−Cu6, blue). Divalent Cu ions are distributed at two substitutional sites of trivalent Bi sites (Bi1(2a) and Bi2(4i)) being substituted in the accreting slab and at four interstitial sites (4i) in nonaccreting slab. Substitutional Cu sites are very close to the neighboring Bi sites (Cu1−Bi1 (0.54 Å), Cu2−Bi2 (1.10 Å)), while the interatomic distances for Cu1−Cu6 (4.0 Å), Cu2−Cu6 (2.98 Å), and Cu1−Cu2 (3.77 Å) are too long. Interstitial Cu sites are statistically distributed in a zigzag pattern around $c = 1/2$ along b-axis. In nonaccreting slab, Cu−Cu bonding along b-axis consisting of Cu3−Cu5 (1.77 Å), Cu5−Cu3 (1.77 Å), and Cu3−Cu3 (1.25 Å) connections in a diamond shape can form an electrical conduction path. In accreting slab, zigzag-shaped bonding between Cu6−Cu6 (2.32 Å) chains can also make another electrical conduction path along b-axis. Thus, the electron conduction might be more favorable in a path parallel to b-axis, suggesting the anisotropy in electrical and electronic thermal conductivities. These directional atomic distributions and bondings between interstitial Cu ions can also induce the

dx.doi.org/10.1021/ic5014945 | Inorg. Chem. 2014, 53, 12732−12738

effective changes in electron conduction and phonon scattering by doping.

(b). Trivalent Substitutional (Bi1 and Bi2) and Divalent Bi Sites (Bi3). Trivalent and divalent Bi sites coexist in the $Cu_{x+y}Bi_{5-y}Se_8$ structure, as shown in Figure 1d. In accreting slab, Bi1 has a nearly regular octahedral coordination, and the marginal Bi2 site is asymmetric. Both trivalent Bi sites are noncoincident with the divalent substitutional Cu ions but share the site occupancy, suggesting the possibility of intensified phonon scattering by increase in effective ionic radius. On the other hand, half of the octahedral divalent Bi3 site in nonaccreting slab possesses the most asymmetric coordination with Bi3−Se5 (2.71 or 3.02 Å) and Bi3−Se2 (2.93 Å). The occupancy of Bi3 site is not changed since this site is not substituted by Cu. There is no Bi−Bi bonding (Bi dimer) observed in this structure.

(c). Divalent Se Site. As shown in Figure 1e, Se atoms are entirely distributed in the unit cell of $Cu_{x+y}Bi_{5-y}Se_8$ by taking the space in the vicinity between Cu and Bi atoms. The only exception is the Se3−Se4 pair with the distance of 0.555 Å that has a bonding to the central Bi1 octahedron. Because of these unique atomic configurations, Se sites can provide effective phonon scattering centers. Structure refinement revealed that the coordination of Se ions could be altered by the change in the configuration of interstitial Cu ions. In particular, the atomic arrangements on each lattice plane along each axis (a-, *b*-, and *c*-axis) are different, resulting in highly asymmetric complex disorders in the unit cell.

Characteristics of Elemental Doping for Each Atomic Site and Electronic Transport Properties. *(a). Cu Site Doping.* In the previous report,[3] it was assumed that interstitial Cu ions acts as a single donor and that n_c could be controlled by variation of Cu/Bi ratio; however, n_c values were varied within the narrow range from 4.56×10^{19} cm^{-3} ($Cu_{1.6}Bi_{4.75}Se_8$) to 7.86×10^{19} cm^{-3} ($Cu_{1.5}Bi_{4.8}Se_8$) for all allowed Cu/Bi ratios. Because S and σ values are determined by the following correlations:

$$S = \frac{8\pi k_B^2}{3eh^2} m^* T \left(\frac{\eta}{3n_c}\right)^{2/3} \quad (1)$$

where k_B is the Boltzmann constant, e is the electron charge, h is the Planck constant, η is the reduced Fermi energy, and $\sigma = n_c e \mu_H$, the control of n_c is the most important and straightforward way to manipulate electronic transport. From the result of Rietveld refinement, in case of impurity doping to Cu sites, it is expected that the dopants are preferentially substituted into the interstitial Cu sites, not into the substitutional ones. To examine the effect of dopants on the n_c, we selected Zn (2+) and In (3+) as doping elements with different charge valences. Figure 3 shows the powder X-ray diffraction (XRD) patterns for pristine and doped $Cu_{1.7}Bi_{4.7}Se_8$ compounds. All patterns are indexed with monoclinic $C2/m$ space group as a major phase, and Bi_2Se_3 as a minor phase was also observed. Additional CuI secondary phase was only observed in $Cu_{1.7}Bi_{4.7}Se_{7.84}I_{0.16}$. As shown in Figure 4, the peak shifts of (1 1 4) reflections to the lower angle are clearly observed in the XRD patterns. The uniformly distributed chemical compositions are also confirmed by energy-dispersive X-ray spectroscopy (EDS) analysis for all doped samples (see Supporting Information, Figure S1). These verify that the dopant ions are well-substituted into the host matrix of Cu−Bi−Se pavonite homologue resulting in the changes of structural parameters such as interplanar distance, interplanar angle, atomic coordinate, and so on. Figure 5a shows the

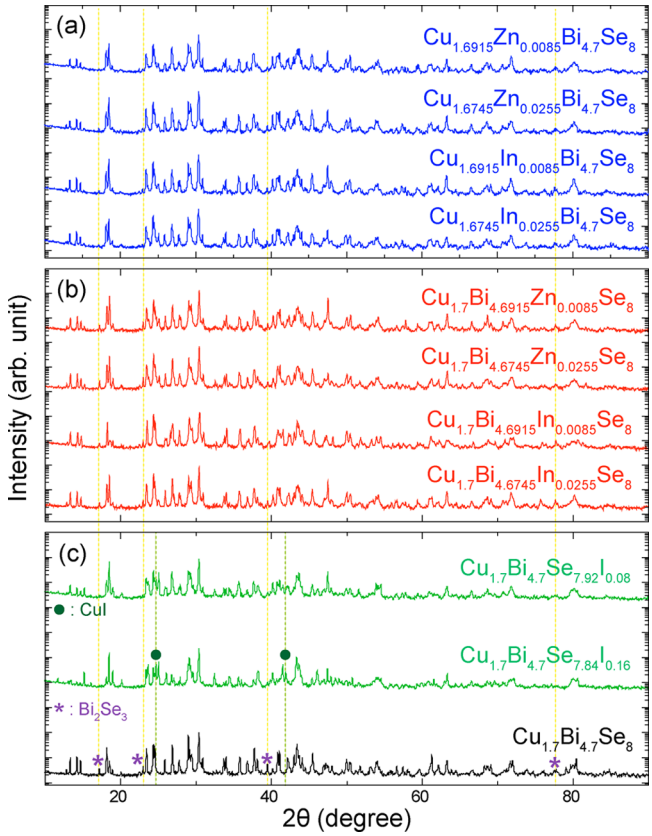

Figure 3. Powder X-ray diffraction patterns of (a) Cu site, (b) Bi site, and (c) Se site modified Cu−Bi−Se structures. Asterisk (*) and circle (●) represent Bi_2Se_3 and CuI secondary phases, respectively.

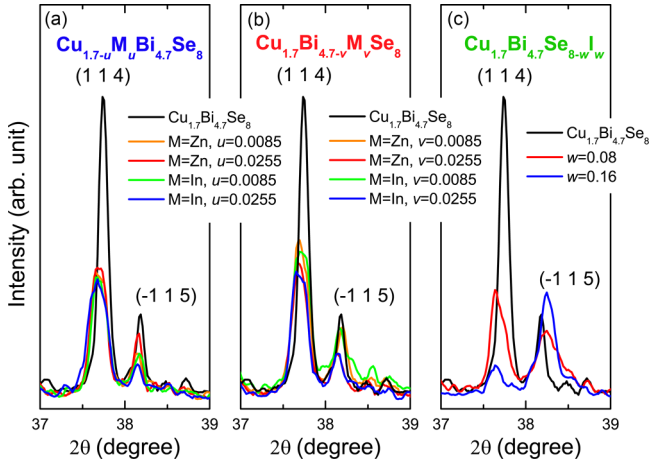

Figure 4. Magnified XRD patterns of the (1 1 4) reflections for (a) $Cu_{1.7-u}M_uBi_{4.7}Se_8$, (b) $Cu_{1.7}Bi_{4.7-v}M_vSe_8$, and (c) $Cu_{1.7}Bi_{4.7}Se_{8-w}I_w$.

temperature dependences of σ and S for pristine and Cu site doped $Cu_{1.7-u}M_uBi_{4.7}Se_8$ (M = Zn and In, u = 0.0085 and 0.0255, respectively) compounds. Cu site doped $Cu_{1.7-u}M_uBi_{4.7}Se_8$ compounds showed the dramatic changes in both σ and S values, indicating the increase in n_c. In spite of the valence difference between Zn^{2+} and In^{3+} dopants, the induced changes in σ and S were similar (Figure 5a,d), which implies that the majority of dopants are at interstitial Cu sites rather than substitutional ones and the electronegativity mismatch provokes the change of electronic transport properties due to the reduced electron negativity (1.65 for Zn and 1.78 for In) compared to Cu

dx.doi.org/10.1021/ic5014945 | Inorg. Chem. 2014, 53, 12732−12738

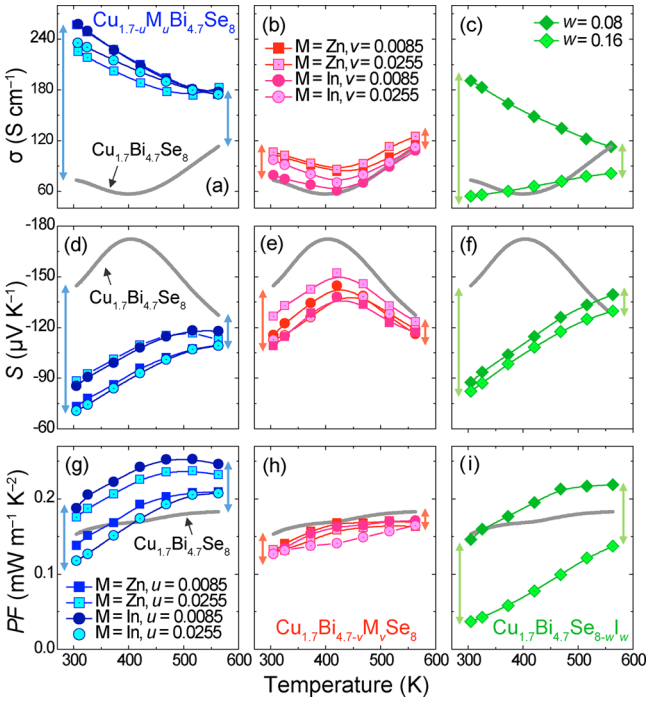

Figure 5. (a–c) Electrical conductivities (σ), (d–f) Seebeck coefficients (S), (g–i) power factors (PF) as a function of temperature for $Cu_{1.7-u}M_uBi_{4.7}Se_8$, $Cu_{1.7}Bi_{4.7-v}M_vSe_8$, $Cu_{1.7}Bi_{4.7}Se_{8-w}I_w$, respectively.

(1.90), resulting in the delocalization of electron density around interstitial Cu site. Note that the PF values of $Cu_{1.6915}In_{0.0085}Bi_{4.7}Se_8$ were higher than those of other compositions over the whole measured temperature range (Figure 5g). This is originated from relatively moderate decrease in S (from −144 to −85 μV K^{-1} at room temperature).

(b). Bi Site Doping. On the basis of the results of Rietveld refinements and the above experiments, we found that n_c could be significantly changed by doping into Cu sites. However, it is conceived that the modification of Bi sites has a moderate effect on electronic transport parameters compared to that of Cu sites. Indeed, the overall changes in σ, S, and PF of Bi site doped $Cu_{1.7}Bi_{4.7-v}M_vSe_8$ compounds are much smaller than those of Cu site doped $Cu_{1.7-u}M_uBi_{4.7}Se_8$. Figure 5b,e shows the temperature dependence of σ and S for pristine and Bi site doped $Cu_{1.7}Bi_{4.7-v}M_vSe_8$ (M = Zn and In, v = 0.0085 and 0.0255, respectively) compounds, exhibiting smaller changes than those of Cu site doped compounds. Further, the shift of onset temperatures for bipolar conduction was relatively lower than those of Cu site doped compounds. This result suggests that the only small increase in n_c was achieved by Zn or In doping on Bi sites. Additionally, the difference in electronegativity between dopants and Bi (electronegativity value of Bi is 2.02) hardly affects the electronic transport due to the delocalized electron density around Bi sites. PF values of Zn- and In-doped compounds were slightly lower than that of $Cu_{1.7}Bi_{4.7}Se_8$, despite increased σ as shown in Figure 5h. We believe that the electronegativity mismatched doping is a more effective way to control both electronic and thermal transport than conventional doping scheme based on the charge imbalance in the complex structures.

(c). Se Site Doping. Figure 5c,f shows the temperature dependence of σ and S for $Cu_{1.7}Bi_{4.7}Se_{8-w}I_w$ (w = 0.08 and 0.16). In case of 1 atom % I-doped composition ($Cu_{1.7}Bi_{4.7}Se_{7.92}I_{0.08}$), σ largely increases, especially at low temperatures. Since the Se ions locate nearby interstitial Cu ions and the atomic distribution of Cu induces the rearrangement of Se, the n_c increases by I doping, leading to the increase in σ and the decrease in S values. However, σ for 2 atom % I-doped compound ($Cu_{1.7}Bi_{4.7}Se_{7.84}I_{0.16}$) decreased. This is related to the formation of secondary phase CuI as shown in Figure 3c, which can reduce μ_H and σ by impurity scattering in spite of the increase of n_c.

In summary, we found that σ was drastically changed by the modification of Cu or Se sites as shown in Figure 5a–c. On the other hand, the region of intrinsic conduction also shifts to higher temperatures with the increase in doping level. This is a typical behavior of degenerated semiconductors induced by the increase in n_c since the increased extrinsic carriers suppress the onset temperature of intrinsic conduction.

Thermal Transport Properties and Thermoelectric Performance. Figure 6 shows the temperature dependences

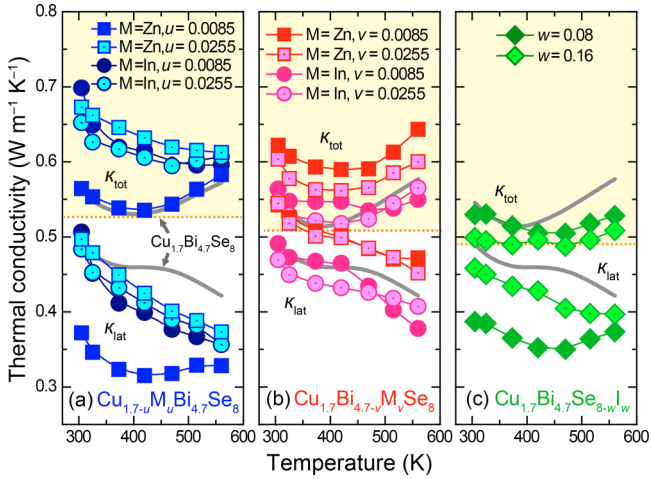

Figure 6. Total thermal conductivity (κ_{tot}) and lattice thermal conductivity (κ_{lat}) as a function of temperature for (a) $Cu_{1.7-u}M_uBi_{4.7}Se_8$, (b) $Cu_{1.7}Bi_{4.7-v}M_vSe_8$, (c) $Cu_{1.7}Bi_{4.7}Se_{8-w}I_w$, respectively.

of total (κ_{tot}), lattice (κ_{lat}), and electronic thermal conductivity (κ_{ele}). We consider that the extremely low thermal conductivities in our samples are an intrinsic property originating from their structural complexities and that the TE contributions by the minor secondary phases (such as, Bi_2Se_3 and CuI) are insignificant, since the values of room temperature thermal conductivities for Bi_2Se_3 and CuI are 3.07 and 1.68 W m^{-1} K^{-1}, respectively,[7] which are much higher values than that of the matrix. We calculated κ_{lat} using the following equation: $\kappa_{tot} = \kappa_{lat} + \kappa_{ele}$, where the κ_{ele} is estimated from the Wiedemann–Franz law, $\kappa_{ele} = L_0T\sigma$. The Lorenz number, L_0, was obtained using following equation:

$$L_0 = \left(\frac{k_B}{e}\right)^2 \left(\frac{\left(r+\frac{7}{2}\right)F_{r+5/2}(\eta)}{\left(r+\frac{3}{2}\right)F_{r+1/2}(\eta)} - \left[\frac{\left(r+\frac{5}{2}\right)F_{r+3/2}(\eta)}{\left(r+\frac{3}{2}\right)F_{r+1/2}(\eta)}\right]^2 \right) \quad (2)$$

where r is the scattering parameter, $F_n(\eta)$ is the Fermi integral of order n, $F_n(\eta) = \int_0^\infty (x^n/(1+e^{(x-\eta)}))dx$, and η is calculated from the value of S, respectively. The value of r, which was derived from the temperature dependence of μ_H, was ~1.5 in the Cu–Bi–Se-based materials, suggesting that the main scattering mechanism was mixed by the interaction between acoustic and optical phonon scatterings of the lattice atoms and/or structural

dx.doi.org/10.1021/ic5014945 | Inorg. Chem. 2014, 53, 12732–12738

defects (point defects).[8,9] Calculated L_0 was nearly constant in all compounds and was in the range of $(2.48-2.58) \times 10^{-8}$ V^2 K^{-2}. The κ_{tot} values increased by doping at Cu and Bi sites due to the increase of the κ_{ele} value. However, the addition of a small amount of iodine decreases κ_{tot} due to the suppression of κ_{lat} by impurity scattering. Interestingly, all κ_{lat} values of Cu site doped compounds ($Cu_{1.7-u}M_uBi_{4.7}Se_8$) were significantly suppressed compared to those of Bi site doped $Cu_{1.7}Bi_{4.7-v}M_vSe_8$. This indicates that the atomic arrangements at interstitial Cu sites are highly related to thermal transport properties and that the doping at interstitial Cu sites is effective to reduce phonon propagation, resulting in the decrease of κ_{lat}. As shown in Figure 6, κ_{lat} was decreased by the modification of each atomic site except for the compositions of $Cu_{1.7}Bi_{4.7-v}Zn_vSe_8$ (v = 0.0085 and 0.0255), mainly due to the mass difference between host ions (Cu, Bi, and Se) and dopants (Zn, In, and I). Room-temperature values of κ_{tot}, ranging from 0.52 to 0.69 W m^{-1} K^{-1}, were found for all compositions. These κ_{tot} values are much lower than those of state-of-the-art low κ_{lat} systems such as Zn_4Sb_3 ($\kappa_{tot} \approx 1.05$ W m^{-1} K^{-1} at 300 K)[10] and $Cu_{2-x}Se$ ($\kappa_{tot} \approx 1$ W m^{-1} K^{-1} at 400 K).[11]

To clarify the role of doping on different atomic sites affecting the thermal transport, we modeled the temperature dependence of the κ_{lat} for pristine, interstitial site-, and substitutional site-doped samples using the Debye−Callaway model[12−21] (see Supporting Information, S4).

As shown in Figure 7, the calculated κ_{lat} is well-matched with experimental data, and impurity scattering prefactor (I) has a strong influence on the κ_{lat}, indicating that the suppression of κ_{lat} is mainly due to the point defect scattering induced by doping. In particular, significant reduction (~34%) in κ_{lat} is observed in the case of the modification of Cu site with Zn ion, decreasing from 0.56 W m^{-1} K^{-1} for undoped sample to 0.37 W m^{-1} K^{-1} for doped compound at 300 K. This is an unexpected result because the mass and the size differences between Cu and isoelectronic Zn are only 2.7% and 5%, respectively. This might be relevant to the preferential occupations of dopants at statistically distributed interstitial Cu sites as well as to the fractional occupancies of those sites in this system. Similar effects of interstitial atoms on structural and TE characteristics were observed in complex structured β-Zn_4Sb_3 and $Cu_{2-x}Se$. Cargnoni et al. demonstrated that Zn interstitial atoms played a fundamental role as electron suppliers to enhance the value of S, as well as to suppress the κ_{lat} value of β-Zn_4Sb_3.[22] Liu et al. showed with first-principle calculations that dopants occupied preferentially the Zn interstitial (or vacancy) sites rather than substitutional ones in β-Zn_4Sb_3 due to the relatively low formation energy.[23] It was also reported that $Cu_{2-x}Se$ showed p-type conduction with a high S and low κ_{lat} due to the ionic and liquid-like behaviors of randomly distributed interstitial Cu ions, respectively.[11] Therefore, considering such correlations between the common structural features and TE properties in three different TE materials with low κ_{lat}, we surmise that the interstitial site ions play a major role to affect TE properties including both thermal and electronic transport characteristics. From σ, S, and κ values, we calculated the ZT values.

Figure 8 shows the temperature dependence of the ZT for pristine and Zn-, and In-doped $Cu_{1.7}Bi_{4.7}Se_8$ ($Cu_{1.7-u}M_uBi_{4.7}Se_8$ (Figure 8a) and $Cu_{1.7}Bi_{4.7-v}M_vSe_8$ (Figure 8b), M = Zn and In, u and v = 0.0085 and 0.0255, respectively), and I-doped $Cu_{1.7}Bi_{4.7}Se_8$ compounds ($Cu_{1.7}Bi_{4.7}Se_{8-w}I_w$ (Figure 7c), w = 0.08 and 0.16). By small amount of In substitution on Cu site, ZT increased owing to the due to the synergetic effects of increase in PF and decrease in κ_{lat}, and the largest ZT value (0.24 at 560 K) was observed for $Cu_{1.6915}In_{0.0085}Bi_{4.7}Se_8$, yielding an enhancement of greater than 30% compared with that of a pristine $Cu_{1.7}Bi_{4.7}Se_8$.

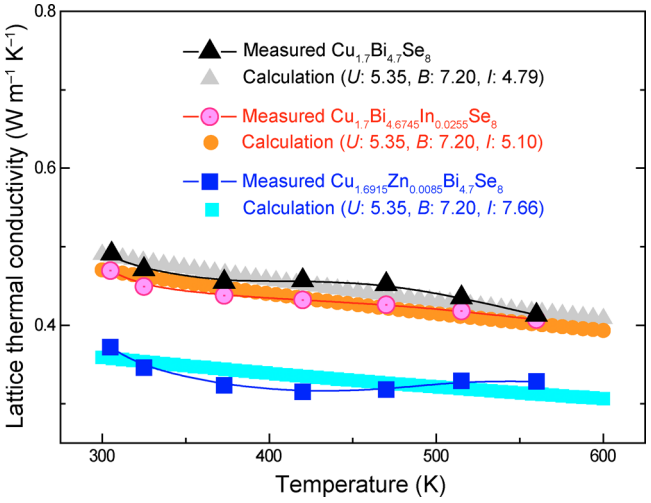

Figure 7. Experimental and calculated lattice thermal conductivity as a function of temperature for $Cu_{1.6915}Zn_{0.0085}Bi_{4.7}Se_8$, $Cu_{1.7}Bi_{4.6745}In_{0.0255}Se_8$, and $Cu_{1.7}Bi_{4.7}Se_8$. In the parentheses, U (10^{-18} s K^{-1}), B (10^7 s^{-1}), and I (10^{-40} s^3) denote scattering prefactors for Umklapp, boundary, and impurity scatterings, respectively.

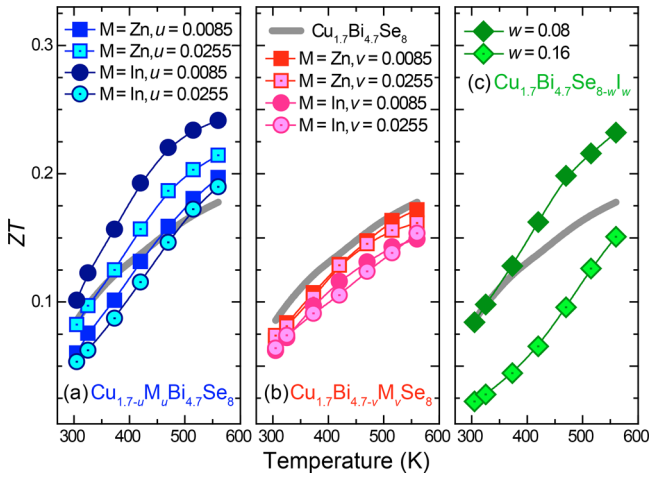

Figure 8. Dimensionless thermoelectric figure of merit (ZT) as a function of temperature for (a) $Cu_{1.7-u}M_uBi_{4.7}Se_8$, (b) $Cu_{1.7}Bi_{4.7-v}M_vSe_8$, (c) $Cu_{1.7}Bi_{4.7}Se_{8-w}I_w$, respectively.

CONCLUSIONS

In this article, we discussed how the electronic and thermal transport characteristics can be manipulated through a variety of strategies involving structural features of each atomic site in complex structured $Cu_{1.7}Bi_{4.7}Se_8$ pavonite homologues. Synchrotron X-ray diffractions and successive Rietveld refinements revealed that this complex structure showed coexistence of substitutional and interstitial Cu sites with fractional occupancies as well as randomly distributed multiple disorders. It is verified that the structural features, including atomic bonding and configurations, are strongly correlated with both electronic and thermal transport properties in this system. In particular, we

dx.doi.org/10.1021/ic5014945 | Inorg. Chem. 2014, 53, 12732−12738

found that σ and κ are significantly affected by the modification of interstitial Cu sites. These indicated that the doping strategy in complexly structured materials should be established based on the understanding of structural characteristics for each atomic site correlated to the physical properties. Furthermore, we suggest that the complex structure composed of interstitial atomic sites may be a guideline for the discovery of promising TE materials.

■ ASSOCIATED CONTENT

Supporting Information

Crystallographic information file (CIF) for the synchrotron X-ray powder diffraction data, lattice thermal conductivity calculation, structural parameters calculated from Rietveld refinements, additional refinement results. This material is available free of charge via the Internet at http://pubs.acs.org.

■ AUTHOR INFORMATION

Corresponding Authors

*E-mail: khlee2014@kangwon.ac.kr. (K.H.L.)
*E-mail: kimsungwng@skku.edu. (S.W.K.)

Author Contributions

◊These authors contributed equally.

Notes

The authors declare no competing financial interest.

■ ACKNOWLEDGMENTS

This work was supported by IBS-R011-D1, the National Research Foundation of Korea (2013R1A1A1008025), the Human Resources Development program (No. 20124010203270) of the Korea Institute of Energy Technology Evaluation and Planning (KETEP) grant funded by the Korea government Ministry of Trade, Industry and Energy.

■ REFERENCES

(1) Snyder, G. J.; Toberer, E. S. *Nat. Mater.* **2008**, *7*, 105.
(2) Wright, D. A. *Nature* **1958**, *181*, 834.
(3) Cho, J. Y.; Mun, H. A.; Ryu, B.; Kim, S. I.; Hwang, S.; Roh, J. W.; Yang, D. J.; Shin, W. H.; Lee, S. M.; Choi, S.-M.; Kang, D. J.; Kim, S. W.; Lee, K. H. *J. Mater. Chem. A* **2013**, *1*, 9768.
(4) Goldsmid, H. J. *J. Appl. Phys.* **1961**, *32*, 2198.
(5) Yang, J.; Meisner, G. P.; Morelli, D. T.; Uher, C. *Phys. Rev. B* **2000**, *63*, 014410.
(6) Rodriguez-Carvajal, J. *Phys. B* **1993**, *192*, 55.
(7) Perry, D. L. *Handbook of Inorganic Compounds*; 2nd ed.; CRC Press: London, U.K., 2011.
(8) Allgaier, R. S.; Scanlon, W. W. *Phys. Rev.* **1958**, *111*, 1029.
(9) Brown, D. M.; Bray, R. *Phys. Rev.* **1962**, *127*, 1593.
(10) Snyder, G. J.; Christensen, M.; Nishibori, E.; Caillat, T.; Iversen, B. B. *Nat. Mater.* **2004**, *3*, 458.
(11) Liu, H.; Shi, X.; Xu, F.; Zhang, L.; Zhang, W.; Chen, L.; Li, Q.; Uher, C.; Day, T.; Snyder, G. J. *Nat. Mater.* **2012**, *11*, 422.
(12) Callaway, J.; Von Baeyer, H. C. *Phys. Rev.* **1960**, *120*, 1149.
(13) Slack, G. A.; Galginaitis, S. *Phys. Rev.* **1964**, *133*, A253.
(14) Glassbrenner, G. A.; Slack, G. A. *Phys. Rev.* **1964**, *134*, A1058.
(15) Morelli, D. T.; Heremans, J. P.; Slack, G. A. *Phys. Rev. B* **2002**, *66*, 195304.
(16) Abeles, B. *Phys. Rev.* **1963**, *131*, 1906.
(17) He, J.; Girard, S.; Kanatzidis, M.; Dravid, V. *Adv. Funct. Mater.* **2010**, *20*, 764.
(18) Pei, Y.; Shi, X.; LaLonde, A. D.; Wang, H.; Chen, L.; Snyder, G. J. *Nature* **2011**, *473*, 66.
(19) Wang, H.; Pei, Y.; LaLonde, A. D.; Snyder, G. J. *Proc. Natl. Acad. Sci. U.S.A.* **2012**, *109*, 9705.
(20) Wang, H.; LaLonde, A. D.; Pei, Y.; Snyder, G. J. *Adv. Funct. Mater.* **2013**, *23*, 1586.
(21) Klemens, P. G. *Solid State Physics;* Academic Press: New York, 1958.
(22) Cargnoni, F.; Nishibori, E.; Rabiller, P.; Bertini, L.; Snyder, G. J.; Christensen, M.; Gatti, C.; Iversen, B. B. *Chem.—Eur. J.* **2004**, *10*, 3861.
(23) Liu, M.; Qin, X.; Liu, C.; Pan, L.; Xin, H. *Phys. Rev. B* **2010**, *81*, 245215.